Seed-Mediated Growth of Uniform Gold Nanoparticle Arrays

ARTICLE *in* THE JOURNAL OF PHYSICAL CHEMISTRY C · AUGUST 2007

Impact Factor: 4.77 · DOI: 10.1021/jp0740393

3 AUTHORS:

Sachin Kumar
Punjab Technical University
11 PUBLICATIONS **263** CITATIONS
SEE PROFILE

Hongzhou Yang
Miami University
26 PUBLICATIONS **1,022** CITATIONS
SEE PROFILE

Shouzhong Zou
American University Washington D.C.
74 PUBLICATIONS **2,443** CITATIONS
SEE PROFILE

Seed-Mediated Growth of Uniform Gold Nanoparticle Arrays

Sachin Kumar, Hongzhou Yang, and Shouzhong Zou*

Department of Chemistry and Biochemistry, Miami University, Oxford, Ohio 45056

Received: May 24, 2007; In Final Form: June 28, 2007

We demonstrated through electron microscopic characterizations that the semi-hexagonal Au nanoparticle arrays supported on solid surfaces prepared by a polymer template approach could be enlarged uniformly by using a solution-based seed-mediated growth. The semi-hexagonal particle arrangement is largely retained after the growth as evident by the similar Fourier transform patterns obtained before and after the growth, indicating that the growth occurs over the seed particles on the surface. The shape and size of the augmented particles can be tuned by varying the growth conditions. The particle density can be conveniently varied by using polymer templates with different chain lengths. The growth mechanism is briefly discussed. Strong surface-enhanced Raman signals of molecules adsorbed on the 40−60 nm grown particles are observed.

Introduction

Two dimension nanoparticle arrays have attracted much attention due to their applications in sensors,[1,2] information storage,[3,4] nanomaterial fabrication,[5−7] bioseparation,[8] and catalysis.[9,10] The particle arrays can be created by different approaches. Among them, electron beam lithography can produce arrays with excellent size, shape, and periodicity control.[9,10] However, the high cost hampers its widespread applications. Self-assembly has been extensively used to assemble nanoparticles made in the solution phase into "superlattices".[11−14] The spacing of the "lattice" can be tuned up to a few nanometers.[14] By depositing metals through ordered nanopores in a template, such as anodic aluminum oxide membranes[15−17] or a layer of close-packed polystyrene beads,[18,19] nanoparticle or nanorod arrays replicating the size and periodicity of the voids/pores can be obtained. In this Article, we report a straightforward solution-based seed-mediated growth approach to fabricate well-ordered two-dimensional arrays of gold nanoparticles with controlled size, shape, and spacing.

Seed-mediated growth of Au nanoparticles in solutions has been well demonstrated.[20,21] In this approach, citrate-capped Au nanoparticles with a diameter of 3−4 nm are prepared in an aqueous solution by the reduction of hydrogen tetrachloroaurate ($HAuCl_4$) with sodium borohydride ($NaBH_4$) in the presence of sodium citrate. These Au particles serve as the growth nuclei (seed) and are enlarged after the addition of a growth solution containing controlled amount of $HAuCl_4$, ascorbic acid (AA), and cetyltrimethylammonium bromide (CTAB). By varying the concentration of the seed and the mole ratio of the ingredients of the growth solution, augmented particles with a desired shape can be obtained.[20,21] Exploiting a similar strategy, several groups have demonstrated the growth of nanorods from citrate-capped Au nanoparticle seeds anchored on surfaces through various molecular linkers.[22−26] Of particular interest is the ability to grow Au nanorods with a preferential orientation on silicon surfaces.[23] Using the Au particles formed directly on indium tin oxide-coated glass slides as the seed, thereby avoiding the complication from the molecular linkers on the electroanalysis applications, Oyama and co-workers showed that these particles can also be enlarged with the seed-mediated growth approach.[27,28] This strategy was recently applied to the growth of Pd nanoparticles by the same group.[29]

Herein, we report fabrication of well-ordered two dimension arrays of gold nanoparticles with controlled size, shape, and spacing by using the seed-mediated growth method. Distinct from the previous studies, in the present work the seed particles form uniform semi-hexagonal arrays with a tunable interparticle spacing from tens to more than a hundred nanometers, and the growth is uniform across a large area. The grown particles register with the seed position and the array pattern is largely intact after the growth, indicating that the growth takes place over the seed particles. By varying the growth solution component concentrations and the seed density, the particle shape can be tailored from triangle to pentagon and hexagon in a fashion similar to the growth of seed particles in the solution.[20,21] The enlarged particles with a diameter of 40−60 nm show strong surface-enhanced Raman scattering activity.

Experimental Section

The fabrication of the seed particle arrays follows the approach developed by Spatz et al., using polystyrene-*b*-poly(2-vinylpyridine) (PS-*b*-P2VP) as a template.[30] Briefly, 25 mg of PS-b-P2VP (Polymer Source Inc., Dorval, Quebec, Canada) was dissolved in 5 mL of dry toluene under vigorous mechanical stirring for at least 5 h. Toluene is a selective solvent for the PS block; therefore, the polymer forms inverse spherical micelles with the P2VP block as the core and the PS block as the corona. Hydrogen tetrachloroaurate trihydrate (Sigma-Aldrich, St. Louis, MO) was used as the metal precursor for forming Au nanoparticles. The metal salt was loaded to the micelles by continuous stirring for at least 48 h. The molar ratio between $HAuCl_4$ and the P2VP unit was 0.2. To obtain different particle densities, polymers with $M_n^{PS} = 25$ and 188 kg mol^{-1}, $M_n^{P2VP} = 15$ and 16 kg mol^{-1}, respectively, were used (denoted as PS(25)-*b*-P2VP(15) and PS(188)-*b*-P2VP(16) correspondingly). Silicon nitride membrane (thickness 100 nm) transmission electron microscopy (TEM) grids from Structure Probe Inc. (West Chester, PA) were used as the substrate, although similar growth was also observed on other substrates, including glass slides,

* To whom correspondence should be addressed. Phone: (513) 529-8084. Fax: (513) 529-5715. E-mail: zous@muohio.edu.

10.1021/jp0740393 CCC: $37.00
Published on Web 08/10/2007

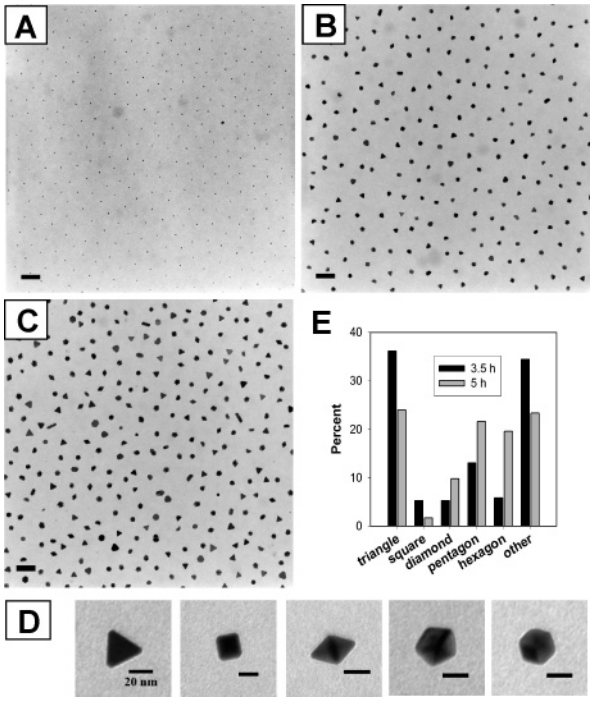

Figure 1. (A−C) TEM images (scale bar: 100 nm) of Au188 nanoparticle arrays on Si_3N_4 membrane: (A) before growth; (B) after 3.5 h growth; (C) after 5 h growth. (D) A closer look of the typical particle shapes observed in (B) and (C). (E) Histograms of shape distribution at different growth times.

indium-tin oxide (ITO)-coated glass slides, and silicon wafers. A monolayer of metal salt containing micelles on silicon nitride TEM grids was formed by dip coating with an immersion rate of 30 mm min^{-1} and a pulling rate of 10 mm min^{-1}. The metal-loaded micelle monolayer covered substrate was subjected to oxygen plasma (100 W, 0.3 Torr) (March Plasma Systems, Concord, CA) for 10 min. The oxygen plasma treatment serves two purposes: first, it reduces the gold salt to form Au particles, and, second, it removes the polymer template from the substrate, as revealed by X-ray photoelectron spectroscopy.[30,31] The substrate temperature does not exceed 100 °C during the oxygen plasma treatment.[30] Prior to the growth, the Au nanoparticle seed arrays were annealed in an oven at 375 °C for 2.5 h.

The growth solution is modified from that described by Sau and Murphy.[21] Briefly, 50 mL of aqueous Au growth solution is prepared by mixing 0.8 mL of 0.1 M CTAB (Sigma-Aldrich, St Louis, MO), 0.1 mL of 0.01 M $HAuCl_4$, and 0.3 mL of 0.1 M AA (Sigma-Aldrich, St Louis, MO). The concentration of each ingredient in this growth solution is 10 times lower than that used in Murphy's work.[21] The substrate with Au nanoparticle array seeds was then immersed in the growth solution at room temperature (25 °C) and kept quiescent for a given time. All glassware used for the growth solution preparation was thoroughly cleaned in aqua regia (3:1 v/v concentrated HCl and HNO_3). (*Caution!* Aqua regia is highly corrosive and toxic, and it should be handled with extreme care.) The glassware was then rinsed in Milli-Q water (Milli-Q A10, Millipore, Bedford, MA) and soaked in water for 1 h prior to use.

TEM images of Au particles and rods were obtained using Zeiss 10C microscope with an accelerating voltage of 100 kV. Scanning electron microscopic (SEM) images were obtained on a Zeiss Supra 35VP FEG microscope. The fast Fourier transform (FFT) analysis was performed using the open source ImageJ program obtained from the NIH website. Image filtering was applied to the raw micrographs to reduce the background interference in the analysis. The background of the FFT pattern was also adjusted to highlight the strongest spots. For particle surface crystal orientation characterization, Pb under potential deposition (UPD) on Au arrays grown on ITO is used.[32,33] Several Pb deposition/desorption cycles were carried out in 0.1 M NaOH + 1 mM $Pb(NO_3)_2$ solution to remove CTAB on the particle surface before the Pb UPD voltammograms were recorded in 0.1 M $HClO_4$ + 1 mM $PbCO_3$ solution.[32,33] Pb UPD experiments were carried out using an electrochemical analyzer (CHI 700B, CH Instuments, TX). A Pt wire served as the counter electrode, and Ag/AgCl (with saturated KCl) was used as the reference electrode.

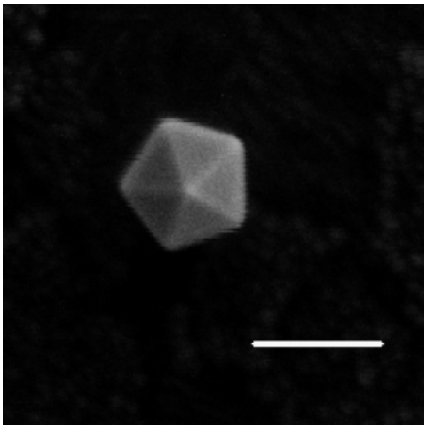

Figure 2. SEM image of a Au pentagon deposited on an ITO-coated glass slide, showing the triangular faces. Scale bar: 200 nm.

SER spectra (SERS) for 1,4-phenylene diisocyanide (PDI) (Sigma-Aldrich, St. Louis, MO) adsorbed on Au nanoparticles were obtained using a micro Raman probe (SpectraCode, West Lafayette, IN) equipped with a SpectraPro 300i monochromator (Acton Research, Acton, MA) and a liquid nitrogen cooled red-intensified back illumination CCD detector (Princeton Instruments, Trenton, NJ). The laser excitation at 785 nm was from a diode laser (Process Instruments, Salt Lake City, UT) coupled to an optical fiber bundle and was focused to a 100 μm spot on the sample with a 20× long working distance microscope objective (NA 0.42). For PDI adsorption on Au nanoparticles, the samples were rinsed with absolute ethanol (Pharmco, Brookfield, CT) followed by immersion in 1 mM PDI ethanol solution for 2 h. Finally, the samples were rinsed sequentially with ethanol and water before Raman measurements.

Results and Discussion

Figure 1A−C shows representative TEM images of the Au particle arrays before (A) and after (B and C) growth. The Au seeds were prepared by using the PS(188)-*b*-P2VP(16) polymer, and the arrays are denoted as Au188. As demonstrated in Figure 1A, the seeds form uniform semi-hexagonal arrays with a 4.5 ± 0.5 nm particle size and ca. 100 nm interparticle distance. The hexagonal symmetry of the arrays is clearly demonstrated by the fast Fourier transform (FFT) power spectrum (Figure S1). The arrays cover the entire grid (0.5 × 0.5 mm). After being immersed for several hours in a growth solution containing 0.02 mM $HAuCl_4$ + 1.6 mM CTAB + 0.6 mM AA (hereafter referred to the standard growth solution), the particles in the arrays are augmented (Figure 1B and C) and the semi-hexagonal pattern is largely retained, as shown by the similar FFT patterns obtained before and after the particle growth (Figure S1). From sample to sample, about 10−15% of the seed particles are missing during the growth, presumably because of the loss of

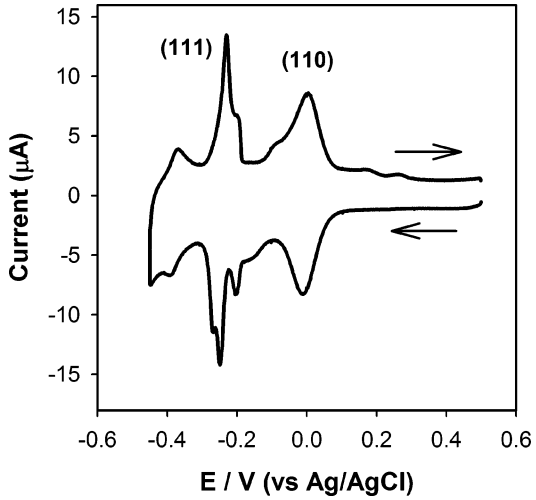

Figure 3. Cyclic voltammogram of Pb UPD on Au188 nanoparticle arrays after being immersed 5 h in the standard growth solution. The particles are supported on an ITO electrode, and the CV was recorded in 1 mM $PbCO_3$ + 0.1 M $HClO_4$. Scan rate: 50 mV s^{-1}. The arrows indicate the scan direction.

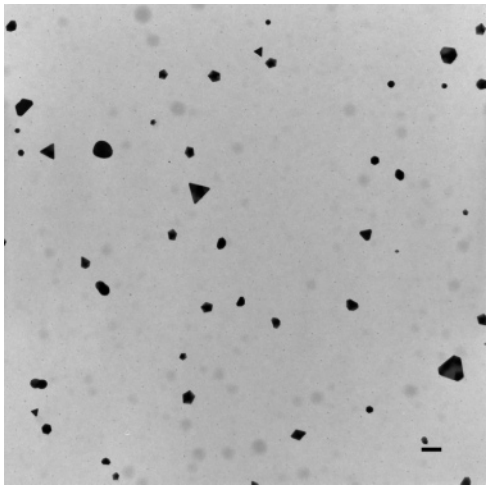

Figure 4. TEM image of Au188 arrays after 2 h growth in the standard growth solution. The seed particles were not annealed. Scale bar: 100 nm. The faint spots are the background features from the silicon nitride grid.

loosely bound particles and the Oswald ripening effect. Nonetheless, the majority of the particles grow into various well-defined shapes, including triangle, square, diamond, pentagon, and hexagon (Figure 1D). The edge length of these particles varies, with the triangles (~30 nm) being the largest and the hexagons being the smallest, about 15 nm. The height of the grown particles is between 9 and 15 nm, as revealed by atomic force microscopy.

The size and height of the overgrown particles depend on the growth time; the initial growth is much faster than the later growth. For example, after 2 h growth the triangles are already in the size range of 20−23 nm. Increasing the growth time to 5 h only enlarges the particles by about 6 nm. This is mainly because of the limited amount (20 μM) of $HAuCl_4$ in the growth solution. Shortening the growth time to 2 h yields a growth pattern similar to that in Figure 1B.

Comparing Figure 1B and C, it is clear that the shape of the particles is better defined with a longer growth time. However, the tradeoff is that the particle size distribution becomes broader (Figure 1C). Smaller particles appear after 5 h growth, due presumably to the Oswald ripening effect. A small amount of the rod-shaped particles with an aspect ratio between 3 and 4 is observed. The particles with different shapes are distributed randomly in the arrays. The histograms in Figure 1E summarize the overall shape distribution. At the shorter growth time, over 60% of the particles have a well-defined shape, and the triangles are dominant. As the growth time increases to 5 h, more than 75% of the particles are well-defined polygons, but the number of the triangles is close to that of the pentagons and hexagons.

From Figure 1D, it is evident that the grown particles are faceted polyhedrons. For example, the pentagon is actually the vertex of an icosahedron with a pentagon base and five triangular faces. This is better seen in a scanning electron microscopic (SEM) image, as shown in Figure 2. However, the exact 3D structure of some of the grown particles is not clear at present. For example, the square could be either a cube or a tetrahedron. Therefore, we name these particles after their shapes in 2D projections. The crystal orientation of the particle faces can be identified empirically by using surface sensitive electrochemical reactions, such as lead underpotential deposition (UPD), as demonstrated recently on the Au nanorods formed by the seed-mediated growth.[33] The faces on the overgrown particles shown in Figure 1 are mainly (111) and (110), as suggested by the voltammogram of lead UPD, which shows a pair of dominant peaks that are characteristic of the (111) and (110) faces (Figure 3). The voltammogram resembles those observed on Au nanorods prepared by the seed-mediated growth of the particles in solutions.[33]

In a control study, TEM grids without the Au seed arrays but undergoing the identical plasma treatment as the samples in Figure 1 were immersed in the standard growth solution for the same length of time. No Au particle was observed, demonstrating the growth is indeed seed mediated. The uniform large-scale growth observed in Figure 1 only occurs after the seed particle arrays are annealed at 375 °C for more than 2 h. Without annealing, only about 10% of the seed particles grow and the overgrown particles are highly polydispersed in size (Figure 4). The ungrown seeds remain on the surface as can be seen from higher magnification images. The annealing probably creates small (111) terraces on the particle surface in a fashion similar to the preparation of the Au(111) thin films by vapor deposition on heated substrates.[34−36] The Pb UPD peaks become sharper after the annealing (Figure S2), suggesting the formation of a more ordered particle surface. The annealing may create a structure that is similar to that of the solution-synthesized seeds, therefore facilitating the growth.

To explore the possibility of tuning the particle shape by changing the amount of the ingredients in the growth solution, we first varied the ascorbic acid (AA) concentration while keeping the growth time and the concentrations of other ingredients the same. With the AA concentration lower than 60 μM, the particle growth is not uniform; only a portion of particles on the substrate grows. With a higher (up to 3 mM) AA concentration, the particle growth is similar to that shown in Figure 1.

Interestingly, doubling the concentration of CTAB to 3.2 mM changes the particle shape distribution significantly: the pentagons and hexagons become dominant, while the triangles become the minority (Figure 5A,B and Figure S3). There is no square or diamond-shaped particle observed. With a prolong growth time, the shape of the particle is better defined and the particles are larger, but the size distribution becomes broader and some inter-connected particles appear (Figure 5B). Increas-

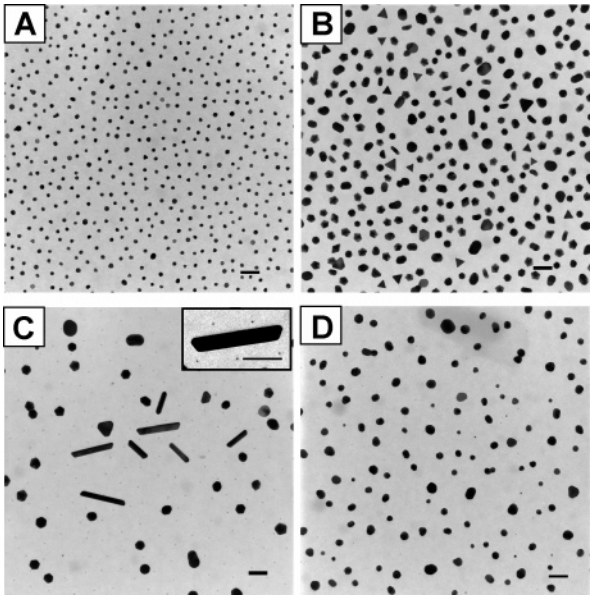

Figure 5. TEM images (scale bar: 100 nm) of Au188 nanoparticle arrays after being immersed in growth solutions containing various amounts of CTAB for 2 h, except for (B), which is grown for 14 h. CTAB concentration: (A, B) 3.2 mM, (C) 16 mM, (D) 100 mM. The inset in (C) is a closer look of a nanorod to clearly show the existence of the seed particles. See text for details.

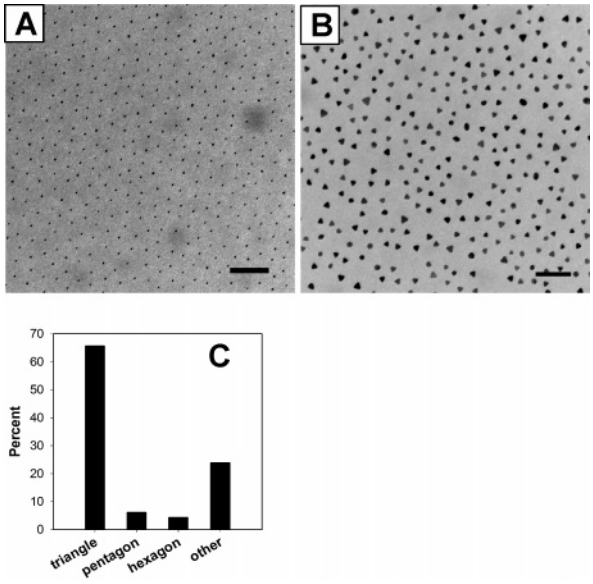

Figure 6. (A,B) TEM images of Au25 nanoparticle arrays before (A) and after 2 h (B) growth. Scale bar: 100 nm. (C) Histograms of particle shape distribution after the growth.

ing the CTAB concentration 10 times to 16 mM leads to the formation of a significant amount of nanorods with a diameter of about 25 nm and an aspect ratio between 5 and 10 (Figure 5C). The growth, however, is not uniform; the majority of the seed particles remain unchanged, especially around the rods (Figure 5C, inset). Further increasing the CTAB concentration to 0.1 M results in the formation of Au nanoparticles with an ill-defined shape and a very broad size distribution (Figure 5D).

We also examined the effect of $HAuCl_4$ concentration. Either increasing or decreasing the gold salt concentration by 5 times does not yield a uniform growth (Figure S4). In the case of a higher $HAuCl_4$ concentration, only a small portion of the Au seed grows rapidly and forms interconnected particle chains. When the gold salt concentration is lower, only two to three enlarged particles are found in an area about 3 μm^2. Both observations suggest the structural difference among the seeds, which may be partly responsible for the growth of particles into different shapes.

As in the growth of seed particles in solutions,[21] another factor that can influence the particle shape is the seed density. By using PS(25)-*b*-P2VP(15), Au nanoparticle arrays (Au25) with the same particle size, but shorter interparticle distance (ca. 40 nm), can be obtained (Figure 6A). Using these particle arrays as the seed and the standard growth solution, an excellent particle growth can also be obtained (Figure 6B). However, a dramatically different particle shape distribution is obtained. More than 65% of the particles are triangular, and the number of pentagons and hexagons is very small (Figure 6C). The semi-hexagonal arrangement of the seed particles is again largely retained after the growth as evident in the FFT power spectrum (Figure S5). The size of the overgrown particles is typically smaller than that of the Au188 arrays under the same growth conditions, which is not unexpected because there are more seeds competing for the same amount of gold source in the Au25 arrays.

At this stage, it is not clear how the particles with different shapes evolve. We speculate that the growth mechanism is in general similar to that of the growth of seeds in the solution. The shape development is likely a result of interplay between the growth kinetics and the adsorption of surfactant on different faces,[21] in a fashion similar to that proposed for explaining the shape control of Pt nanoparticles.[37,38] In a recent study, through monitoring the seed-mediated growth of nanorods from Au nanoparticles attached to lysine-modified Si(100) surfaces, Liao and Hafner[22] showed that the mechanism for particle growth on surfaces follows that for the growth of particles in the solution proposed by Murphy and co-workers.[20,39]

We notice that there are also some differences between the growth of particles on surfaces and that of the particles in the solution. For example, the mole ratio of $HAuCl_4$, CTAB, and AA in the standard growth solution is the same as that used by Sau and Murphy for the growth of square particles in the solution.[21] On the surface, however, the triangle is the dominant shape, and the square is always the minority (Figure 1). The diamonds and the pentagons seen in Figure 1 were not observed in the growth of particles in the solution. These differences may come from various sources. First, the structure of the seed particles prepared by the plasma approach used here may be different from that of the particles made in the solution; second, the diffusion of the Au source to the supported seed particles can be very different from that in the solution; third, the presence of the solid support may promote the horizontal growth. To fully understand the growth mechanism requires more systematic work.

As mentioned in the Introduction, the seed-mediated growth of supported Au nanoparticles to form nanorods and larger nanoparticles has been reported.[22−28] As compared to these previous studies, this work is different in that the seed particles form uniform semi-hexagonal arrays, and this pattern remains after the growth as evident by the Fourier transform pattern. In addition, the seed particle density can be conveniently varied by using polymers with a different polystyrene block length, and the overgrown particles are well separated from each other. These spatial distribution advantages facilitate our further understanding of the growth mechanism of supported particles. In the previous studies where the seed particles are attached to the surfaces through molecular anchoring groups, the particle registration is not controlled. The origin of the grown particles

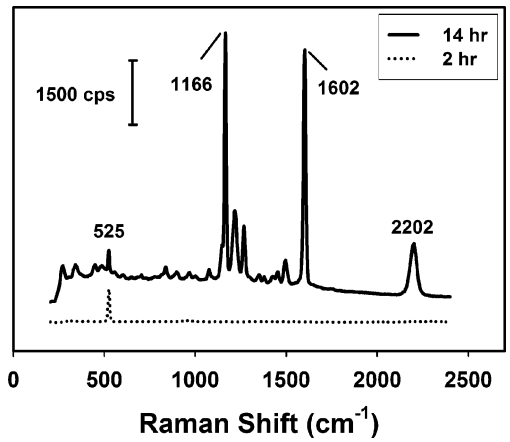

Figure 7. Surface-enhanced Raman spectra of 1,4-phenylene diisocyanide adsorbed on Au nanoparticles after 2 h (bottom trace) and 14 h (top trace) growth. Spectral acquisition time 10 s. Laser excitation: 785 nm. Spectral resolution: 5 cm^{-1}. The 525 cm^{-1} band is the phonon mode of the silicon support.

can be ambiguous. They can be formed through either (1) the growth of the original surface-attached Au nanoparticle seeds or (2) the growth of the new seeds in the solution or on the surface whose formation is catalyzed by the original Au nanoparticle seeds.[22,40] Such an ambiguity is absent in the present study. The retention of the semi-hexagonal pattern indicates that the second growth path is insignificant.

The ultimate goal of the present work is to create arrays of nanoparticles with uniform size and shape by the seed-mediated growth. Although the particle shape control is not yet optimized at present, the ability of tuning the particle shape and size by varying the growth conditions is nonetheless demonstrated and particularly attractive. These particle arrays will find applications in various research areas, such as surface-enhanced Raman spectroscopy (SERS),[1,2,41] catalysis,[9,10] and bioseparation.[8]

To illustrate the application of these particle arrays in SERS, we used 1,4-phenylene diisocyanide (PDI) as a probe molecule. PDI is known to strongly adsorb on Au and Pt-group transition metals.[42,43] A set of Raman spectra obtained on the particle arrays shown in Figure 5A and B are displayed in Figure 7. The particles after 14 h growth show very strong SERS signals characteristics of PDI adsorbed on Au,[42,43] yet the smaller particles obtained after 2 h growth do not yield detectable PDI signal. The size of the particles after 14 h growth is in the range of 40−60 nm, which is known to yield strong SERS signals with a 785 nm excitation.[44]

Conclusions

We have shown that by utilizing the solution-based seed-mediated growth, the uniform arrays of Au nanoparticles prepared by a polymer template approach can be enlarged with a reasonably good control of particle shape and size. The seed array pattern is largely retained after the growth. The grown particle arrays can be used as SERS substrates. Applications of these overgrown particle arrays in SERS and other research areas, including catalysis, nanomaterial fabrication, and bio-separation, are being explored.

Acknowledgment. Financial support from the National Science Foundation (CHM 0616436) and Research Corporation (RI 1218) is greatly appreciated. We thank Dr. Richard Edelmann of Miami University Electron Microscopy Facility for his assistance in acquiring TEM images and the Pacey group for the use of their oven.

Supporting Information Available: Histograms of the particle shape distribution of Au188 arrays after being immersed in 3.2 mM CTAB + 0.02 mM $HAuCl_4$ + 0.6 mM AA, CVs of Pb UPD on Au25 arrays before and after annealing, FFT power spectra of particle arrays before and after growth, and TEM images of Au188 arrays after being immersed in growth solutions with various amounts of Au salt. This material is available free of charge via the Internet at http://pubs.acs.org.

References and Notes

(1) Haes, A. J.; Chang, L.; Klein, W. L.; Van Duyne, R. P. *J. Am. Chem. Soc.* **2005**, *127*, 2264−2271.
(2) Haes, A. J.; Van Duyne, R. P. *Anal. Bioanal. Chem.* **2004**, *379*, 920−930.
(3) Chen, M.; Kim, J.; Liu, J. P.; Fan, H. Y.; Sun, S. H. *J. Am. Chem. Soc.* **2006**, *128*, 7132−7133.
(4) Sun, S. H. *Adv. Mater.* **2006**, *18*, 393−403.
(5) Gao, D.; He, R. R.; Carraro, C.; Howe, R. T.; Yang, P. D.; Maboudian, R. *J. Am. Chem. Soc.* **2005**, *127*, 4574−4575.
(6) Greyson, E. C.; Babayan, Y.; Odom, T. W. *Adv. Mater.* **2004**, *16*, 1348−1352.
(7) Lu, J. Q.; Yi, S. S. *Langmuir* **2006**, *22*, 3951−3954.
(8) Li, B. Q.; Fang, X. H.; Luo, H. B.; Seo, Y. S.; Petersen, E.; Ji, Y.; Rafailovich, M.; Sokolov, J.; Gersappe, D.; Chu, B. *Anal. Chem.* **2006**, *78*, 4743−4751.
(9) Contreras, A. M.; Grunes, J.; Yan, X. M.; Liddle, A.; Somorjai, G. A. *Top. Catal.* **2006**, *39*, 123−129.
(10) Kwon, S.; Yan, X. M.; Contreras, A. M.; Liddle, J. A.; Somorjai, G. A.; Bokor, J. *Nano Lett.* **2005**, *5*, 2557−2562.
(11) Daniel, M. C.; Astruc, D. *Chem. Rev.* **2004**, *104*, 293−346.
(12) Kim, B.; Tripp, S. L.; Wei, A. *J. Am. Chem. Soc.* **2001**, *123*, 7955−7956.
(13) Maye, M. M.; Lim, I. I. S.; Luo, J.; Rab, Z.; Rabinovich, D.; Liu, T. B.; Zhong, C. J. *J. Am. Chem. Soc.* **2005**, *127*, 1519−1529.
(14) Schadt, M. J.; Cheung, W.; Luo, J.; Zhong, C. J. *Chem. Mater.* **2006**, *18*, 5147−5149.
(15) Kline, T. R.; Tian, M. L.; Wang, J. G.; Sen, A.; Chan, M. W. H.; Mallouk, T. E. *Inorg. Chem.* **2006**, *45*, 7555−7565.
(16) Martin, C. R. *Chem. Mater.* **1996**, *8*, 1739−1746.
(17) Yao, J. L.; Pan, G. P.; Xue, K. H.; Wu, D. Y.; Ren, B.; Sun, D. M.; Tang, J.; Xu, X.; Tian, Z. Q. *Pure Appl. Chem.* **2000**, *72*, 221−228.
(18) Haynes, C. L.; McFarland, A. D.; Smith, M. T.; Hulteen, J. C.; Van Duyne, R. P. *J. Phys. Chem. B* **2002**, *106*, 1898−1902.
(19) Haynes, C. L.; Van Duyne, R. P. *J. Phys. Chem. B* **2001**, *105*, 5599−5611.
(20) Murphy, C. J.; San, T. K.; Gole, A. M.; Orendorff, C. J.; Gao, J. X.; Gou, L.; Hunyadi, S. E.; Li, T. *J. Phys. Chem. B* **2005**, *109*, 13857−13870.
(21) Sau, T. K.; Murphy, C. J. *J. Am. Chem. Soc.* **2004**, *126*, 8648−8649.
(22) Liao, H. W.; Hafner, J. H. *J. Phys. Chem. B* **2004**, *108*, 19276−19280.
(23) Mieszawska, A. J.; Slawinski, G. W.; Zamborini, F. P. *J. Am. Chem. Soc.* **2006**, *128*, 5622−5623.
(24) Mieszawska, A. J.; Zamborini, F. P. *Chem. Mater.* **2005**, *17*, 3415−3420.
(25) Taub, N.; Krichevski, O.; Markovich, G. *J. Phys. Chem. B* **2003**, *107*, 11579−11582.
(26) Mieszawska, A. J.; Jalilian, R.; Sumanasekera, G. U.; Zamborini, F. P. *J. Am. Chem. Soc.* **2005**, *127*, 10822−10823.
(27) Zhang, J.; Kambayashi, M.; Oyama, M. *Electrochem. Commun.* **2004**, *6*, 683−688.
(28) Zhang, J. D.; Oyama, M. *Anal. Chim. Acta* **2005**, *540*, 299−306.
(29) Chang, G.; Oyama, M.; Hirao, K. *J. Phys. Chem. B* **2006**, *110*, 20362−20368.
(30) Spatz, J. P.; Mossmer, S.; Hartmann, C.; Moller, M.; Herzog, T.; Krieger, M.; Boyen, H. G.; Ziemann, P.; Kabius, B. *Langmuir* **2000**, *16*, 407−415.
(31) Kastle, G.; Boyen, H. G.; Weigl, F.; Ziemann, P.; Riethmuller, S.; Hartmann, C. H.; Spatz, J. P.; Moller, M.; Garnier, M. G.; Oelhafen, P. *Phase Transit.* **2003**, *76*, 307−313.
(32) Hernandez, J.; Solla-Gullon, J.; Herrero, E. *J. Electroanal. Chem.* **2004**, *574*, 185−196.
(33) Hernandez, J.; Solla-Gullon, J.; Herrero, E.; Aldaz, A.; Feliu, J. M. *J. Phys. Chem. B* **2005**, *109*, 12651−12654.

(34) Derose, J. A.; Lampner, D. B.; Lindsay, S. M.; Tao, N. J. *J. Vac. Sci. Technol., A* **1993**, *11*, 776−780.
(35) Hwang, J.; Dubson, M. A. *J. Appl. Phys.* **1992**, *72*, 1852−1857.
(36) Semaltianos, N. G.; Wilson, E. G. *Thin Solid Films* **2000**, *366*, 111−116.
(37) Petroski, J. M.; Wang, Z. L.; Green, T. C.; El-Sayed, M. A. *J. Phys. Chem. B* **1998**, *102*, 3316−3320.
(38) Wang, Z. L. *J. Phys. Chem. B* **2000**, *104*, 1153−1175.
(39) Johnson, C. J.; Dujardin, E.; Davis, S. A.; Murphy, C. J.; Mann, S. *J. Mater. Chem.* **2002**, *12*, 1765−1770.
(40) Wei, Z.; Mieszawska, A. J.; Zamborini, F. P. *Langmuir* **2004**, *20*, 4322−4326.
(41) Tian, Z. Q.; Ren, B.; Wu, D. Y. *J. Phys. Chem. B* **2002**, *106*, 9463−9483.
(42) Jaiswal, A.; Tavakoli, K. G.; Zou, S. Z. *Anal. Chem.* **2006**, *78*, 120−124.
(43) Gruenbaum, S. M.; Henney, M. H.; Kumar, S.; Zou, S. Z. *J. Phys. Chem. B* **2006**, *110*, 4782−4792.
(44) Wei, A.; Kim, B.; Sadtler, B.; Tripp, S. L. *ChemPhysChem* **2001**, *2*, 743−745.